Cloning and Characterization of Mouse Nucleoside Triphosphate Diphosphohydrolase-8[†,‡]

François Bigonnesse,[§,||] Sébastien A. Lévesque,[§,||] Filip Kukulski,[§] Joanna Lecka,[§] Simon C. Robson,[⊥] Maria J. G. Fernandes,[§] and Jean Sévigny*[,§]

Centre de recherche en Rhumatologie et Immunologie, Université Laval, Sainte-Foy, Québec, Canada, and Department of Medicine, Beth Israel Deaconess Medical Center, Harvard Medical School, Boston, Massachusetts 02215

Received December 10, 2003; Revised Manuscript Received February 17, 2004

ABSTRACT: A novel mammalian plasma membrane bound nucleoside triphosphate diphosphohydrolase (NTPDase), named NTPDase8, has been cloned and characterized. Analysis of cDNA reveals an open reading frame of 1491 base pairs encoding a protein of 497 amino acid residues with an estimated molecular mass of 54650 Da and a predicted isoelectric point of 5.94. In a mouse, the genomic sequence is located on chromosome 2A3 and is comprised of 10 exons. The deduced amino acid sequence reveals eight putative N-glycosylation sites, two transmembrane domains, five apyrase-conserved regions, and 20−50% amino acid identity with other mammalian NTPDases. mRNA expression was detected in liver, jejunum, and kidney. Both intact cells and crude cell lysates from COS-7 cells expressing NTPDase8 hydrolyzed P2 receptor agonists, namely, ATP, ADP, UTP, and UDP, but did not hydrolyze AMP. There was an absolute requirement for divalent cations for the catalytic activity ($Ca^{2+} > Mg^{2+}$) with an optimal pH between 5.5 and 8.0 for ATP and 6.4 for ADP hydrolysis. Kinetic parameters derived from analysis of crude cell lysates showed that the enzyme had lower apparent K_m values for adenine nucleotides and for triphosphonucleosides ($K_{m,app}$ of 13 μM for ATP, 41 μM for ADP, 47 μM for UTP, and 171 μM for UDP). Hydrolysis of triphosphonucleosides resulted in a transient accumulation of the corresponding diphosphonucleoside, as expected from the apparent K_m values. Enzymatic properties of NTPDase8 differ from those of other NTPDases suggesting an alternative way to modulate nucleotide levels and consequently P2 receptor activation.

Ecto-nucleoside triphosphate diphosphohydrolase (E-NTPDase)[1] describes a family of mammalian enzymes that catalyze the hydrolysis of γ- and β-phosphate residues of nucleotides, albeit with different abilities (*1*). These enzymes require divalent cations (Ca^{2+} and/or Mg^{2+}) for full enzymatic activity. They are tightly bound to the plasma membrane and/or to intracellular organelles by one or two transmembrane domains. The catalytic site of NTPDases faces the extracellular milieu (NTPDase1−3) and/or the lumen of intracellular organelles such as the Golgi apparatus and endoplasmic reticulum (NTPDase4−7). NTPDase5 and 6 may also be found on the plasma membrane and secreted following proteolytic cleavage (*2*). Members of this family of enzymes share five apyrase-conserved regions (ACRs). NTPDases have been described under various names in the past (*1*): NTPDase1 (CD39, ATPDase, ecto-apyrase) (*3*−*5*), NTPDase2 (CD39L1, ecto-ATPase) (*6*−*9*), NTPDase3 (CD39L3, HB6) (*10*, *11*), NTPDase4 (UDPase, LALP70) (*12*, *13*), NTPDase5 (CD39L4, ER-UDPase, PCPH) (*2*, *14*, *15*), and NTPDase6 (CD39L2) (*16*−*18*). Another member found recently and named LALP1 may also be considered as NTPDase7 (*19*).

The presumptive role of plasma membrane bound NTPDases, more specifically NTPDase1−3, is to regulate the concentration of extracellular nucleotides and thereby modulate their biological effects exerted by the activation of numerous P2Y and P2X receptors. A few functions have been demonstrated in vivo for NTPDase1. It is a key player in the ability of vascular endothelium to block platelet aggregation by clearing ADP from the blood (*4*, *20*−*24*). Interestingly, NTPDase1 activity is also necessary to keep platelets functional by preventing $P2Y_1$ receptor desensitization at their surface (*23*). More recently, NTPDase1 was shown to be expressed on Langerhans cells, where it plays a complex role in inflammation and immunity (*25*). An opposing function to NTPDase1 has been demonstrated in vitro for NTPDase2. The latter ectonucleotidase facilitates platelet aggregation by generating ADP in the presence of

[†] This work was supported by grants from the Canadian Institutes of Health Research (CIHR; MOP-49460, M2C-50334) and the Fonds de la Recherche en Santé du Québec (FRSQ; 2822) to J.S. At the beginning of this work, J.S. received a Scholarship from the American Liver Foundation.

[‡] The GenBank accession number for mouse *Entpd8* is AY364442.

* To whom correspondence should be addressed: Centre de recherche en Rhumatologie et Immunologie, Centre hospitalier de l'Université Laval, Room T1-49, Ste-Foy (Québec), Canada G1V 4G2. Tel.: (418) 656-4141 ext. 46319. Fax: (418) 654-2765. E-mail: jean.sevigny@crchul.ulaval.ca.

[§] Université Laval.

[||] Equally contributed.

[⊥] Harvard Medical School.

[1] Abbreviations: ACR, apyrase-conserved regions; EST, expressed sequence tag; HPLC, high-performance liquid chromatography; NTPDase, nucleoside triphosphate diphosphohydrolase; PCR, polymerase chain reaction; RT, reverse transcription; SSC buffer, sodium chloride−sodium citrate buffer; UV, ultraviolet light.

10.1021/bi0362222 CCC: $27.50
Published on Web 04/13/2004

ATP (*26*). Also of significant physiological importance is the final conversion of the NTPDase end product AMP to adenosine by ecto-5′-nucleotidase. Adenosine exerts various biological effects that often contrast with the functions of P2 receptors. For example, adenosine has antiaggregatory and anti-inflammatory properties (*27*).

These observations indicate the importance of tightly regulating extracellular nucleotide and nucleoside levels. To date, 15 functional P2 receptors (*28*−*31*) as well as 4 subtypes of adenosine receptors (*27*, *32*) have been cloned and characterized. Because these receptors are expressed in all mammalian tissues, it emphasizes the need for specific enzymes that control the nucleotide/nucleoside levels at the cell surface.

In this paper, we report the identification and characterization of a fourth plasma membrane bound NTPDase with distinct biochemical properties that we have named NTPDase8.

EXPERIMENTAL PROCEDURES

Materials. Agarose, aprotinin, ethylenediaminetetraacetic acid (EDTA), ethylene glycol bis(2-aminoethyl ether)-*N*,*N*,*N*′,*N*′-tetraacetic acid (EGTA), 2-(4-morpholino)ethanesulfonic acid (MES), nucleotides, phenylmethanesulfonyl fluoride (PMSF), sodium acetate, tetrabutylammonium hydrogen sulfate (TBA), and tris(hydroxymethyl)aminomethane (Tris) were purchased from Sigma−Aldrich (Oakville, Canada). Glycine was provided by Fisher Scientific Ltd. (Nepean, Canada). All cell culture media were obtained from Invitrogen (Burlington, Canada), and the 24-well plates were obtained from VWR Canlab (Mont-Royal, Canada).

RT-PCR Cloning. Total RNA was isolated from various mouse tissues, as indicated in Figure 3, with Trizol reagent (Invitrogen). cDNA was synthesized with SuperScript II (Invitrogen) from 500 ng of the total RNA with oligo $(dT)_{18}$ as the primer, according to the instructions of the manufacturer (Invitrogen). For amplification, one-fifth of the reverse transcription (RT) reaction volume was used as a template in a final volume of 50 μL, containing 0.4 μM primer, 200 μM dNTP, and 0.7 unit of Tgo DNA polymerase (Roche, Laval, Canada). The two following sets of primers were designed based on the 5′ and 3′ ends of incomplete mouse ESTs (GenBank accession numbers BB610017 and AV026718, respectively): (1st set) forward 5′GGA-GAC-GGG-GTG-TGG-AGG-AC3′, reverse 5′GGG-GTT-CAT-AAG-GGC-AGG-CA3′; (2nd set) forward 5′GTA-GGT-GGA-GAC-GGG-GTG-TG3′, reverse 5′GGG-TTC-ATA-AGG-GCA-GGC-AT3′. Amplification was started with 2 min at 94 °C followed by 35 cycles of denaturation for 1 min at 94 °C, annealing for 2 min at 60 °C, and primer extension for 2 min at 72 °C and ended with incubation for 7 min at 72 °C. As a control, glyceraldehyde dehydrogenase (GAPDH) amplification was used as described previously (*33*). The PCR product of approximately 1.8 kb obtained from liver was purified on a 1% agarose gel using the QIAEX II gel extraction kit (Qiagen, Mississauga, Canada) and ligated to pcDNA3.1/V5-His (Invitrogen). Plasmid DNA was purified with the QIAprep Spin Miniprep kit (Qiagen), and the orientation of the insert was determined by restriction-enzyme mapping. Two independent clones (one for each set of primers) with the orientation allowing the expression of the protein were amplified and sequenced. One clone was completely sequenced in both directions and the second clone in one orientation to confirm the sequence obtained from the first clone. Both sequences were identical.

Northern Blot Analysis. Northern blot analysis was performed with total RNA from various mouse tissues extracted as described above. RNA (20 μg) was size-fractionated by electrophoresis on a 1% agarose gel containing 10% formaldehyde and transferred to a Hybond-N^+ membrane (Amersham Pharmacia Biotech, Oakville, Canada). The membrane was dehydrated at 37 °C for 30 min, prehybridized with the hybridization buffer (5× SSC, 5× Denhardt's solution, 50 mM NaH_2PO_4, 0.1% sodium pyrophosphate, 0.5% SDS, 200 μg/mL salmon sperm DNA, and 50% formamide), and hybridized with a ^{32}P-labeled cDNA probe in the same buffer not containing the Denhardt's solution. The 470-bp fragment generated by the digestion of the plasmid containing mouse NTPDase8 cDNA with *Bst*XI was used as a probe. Next, the membrane was rinsed with the washing buffer (0.1% SDS and SSC) containing decreasing concentrations of SSC (1×, 0.2×, and 0.1×) and exposed to X-ray film (Eastman Kodak, Rochester, NY).

Genomic Characterization of Entpd8. The NTPDase8 cDNA sequence was used to search the National Center for Biotechnology Information (NCBI) mouse genome database. The sequence identified as NT_039205 showed 100% homology with mouse NTPDase8 cDNA. Oligos were designed to clone the genomic sequence of mouse *Entpd8* into two fragments. PCR products were obtained from mouse genomic DNA (*34*) with the following primers: (1) forward 5′CTG-CTG-TCC-ACT-TCA-CCC-TT3′, reverse 5′TCC-CGC-CCA-AAG-CAG-AGG-TA3′; (2) forward 5′CAA-GAG-ACA-TCC-TAG-CTG-CA3′, reverse 5′GGG-GTT-CAT-AAG-GGC-AGG-CA3′. The two fragments of 1.9 and 2.1 kb were purified on an agarose gel and cloned into pcDNA3.1/V5-His. Plasmids were identified by colony hybridization using a primer labeled with [γ-^{32}P]ATP (PerkinElmer Life Sciences, Woodbridge, Canada) and purified as described above. Selected clones were sequenced, and exon/intron junctions were analyzed with NCBI BLAST.

Cell Transfection and Protein Preparation. COS-7 cells were transfected in 10-cm plates using Lipofectamine (Invitrogen), as previously described (*4*). Briefly, cells were incubated for 5 h at 37 °C in Dulbecco's modified Eagle's medium (DMEM) in the absence of fetal bovine serum (FBS) with 6 μg of plasmid DNA and 24 μL of Lipofectamine reagent. The reaction was stopped by adding an equal volume of DMEM containing 20% FBS, and cells were harvested 40−44 h later. For protein−lysate preparation, transfected cells were washed 3 times with Tris-saline buffer at 4 °C, harvested by scraping in the harvesting buffer (95 mM NaCl, 0.1 mM PMSF, and 45 mM Tris at pH 7.5), and washed twice by centrifuging at 300*g* for 10 min at 4 °C. Cells were resuspended in the harvesting buffer containing 10 μg/mL aprotinin and sonicated. Nuclei and cellular debris were discarded by centrifuging at 300*g* for 10 min at 4 °C, and the supernatants, indicated in the text as crude cell lysates, were stored at −80 °C until used. Protein concentration was estimated by the Bradford microplate assay using bovine serum albumin (BSA) as a standard (*35*).

NTPDase Activity Measurement. Enzyme activity in the protein fractions was determined as previously described (*5*).

Briefly, enzyme activity was measured at 37 °C in 0.5 mL of the following incubation medium: 5 mM $CaCl_2$ either with 100 mM Tris at pH 7.4 or with 100 mM MES at pH 6.4 or as indicated. Crude cell lysates were added to the incubation mixture and preincubated at 37 °C for 3 min. The reaction was initiated by the addition of 0.5 mM nucleotide (ATP, ADP, UTP, UDP, or AMP) and stopped after 20 min with 0.125 mL of malachite green reagent (*36*). Activity on intact COS-7 and 293T cells was determined under similar conditions in 24-well plates, with the addition of 145 mM NaCl to the incubation medium. The reaction was stopped by sampling an aliquot of 0.2 mL and rapidly mixing with 50 μL of malachite reagent. The inorganic phosphate (P_i) released from the hydrolysis of exogenous nucleotides was measured according to Baykov et al. (*36*). For all experiments, enzyme activity was assayed 40−44 h after transfection.

The optimum pH for enzyme activity was determined in the presence of 5 mM $CaCl_2$ with the following buffers: 100 mM acetate (pH 4.0−5.5), 100 mM MES (pH 5.5−7.0), 100 mM Tris (pH 7.0−9.0), or 100 mM glycine (pH 9.0−11.0). In some experiments, $CaCl_2$ was substituted by $MgCl_2$. To remove traces of divalent cations, 1 mM EDTA and 1 mM EGTA were added to the medium. One unit of enzyme activity corresponds to the release of 1 μmol of P_i/min at 37 °C (*37*). Specific activity was expressed as units per well or per milligram of proteins, as indicated. All experiments were performed 3 times with the appropriate controls.

Separation and Quantification of Nucleotides by HPLC. For HPLC analysis, activity assays were performed in 5 mM $CaCl_2$ and 100 mM MES at pH 6.4 as described above with the following modifications. Aliquots of 20 μL were taken at different time points from the enzymatic reaction, and activity was stopped by the addition of an equal volume of ice-cold 1 M perchloric acid. The samples were centrifuged at 1000*g* for 5 min at 4 °C. Supernatants were neutralized with 1 M KOH (4 °C) and centrifuged for a subsequent 5 min at 1000*g*, and the lipids were removed by liquid−liquid extraction with *n*-heptane (5:1, v/v). An aliquot of 20 μL from the lipid-extracted sample was applied to a column connected to a HPLC system.

Adenine nucleotides (ATP, ADP, and AMP) were separated on a 15 cm × 4.6 mm, 3 μm SUPELCOSIL LC-18-T column (Supelco, Bellefonte, PA) with a mobile phase composed of 25 mM TBA, 5 mM EDTA, 100 mM KH_2PO_4/K_2HPO_4 at pH 7.0, and 2% (v/v) methanol, at a flow rate of 1 mL/min. Uracil nucleotides (UTP, UDP, and UMP) were resolved using the SUPELCOSIL LC-18-T column (25 cm × 4.6 mm, 5 μm, Supelco) as described above with the difference that the mobile phase did not contain methanol. Combined adenine and uracil nucleotide samples were analyzed with the latter column with a mobile phase composed of 16.7 mM TBA, 3.3 mM EDTA, and 66.7 mM KH_2PO_4/K_2HPO_4 at pH 7.0. The flow rate was 0.5 mL/min for the first 20 min and 1 mL/min for up to 90 min. The nucleotides were detected by UV absorption at 260 nm and identified by comparing the retention time and UV spectrum with the appropriate standards.

RESULTS

Cloning and Characterization of Mouse NTPDase8 cDNA. The open reading frame of mouse NTPDase8 spans 1491 nucleotides encoding a protein of 497 amino acid residues with a predicted molecular mass of 54650 Da and a calculated isoelectric point of 5.94. The deduced amino acid sequence contains eight potential N-glycosylation sites, all five apyrase-conserved regions, and various putative phosphorylation sites, including one for both protein kinase C and casein kinase II on serine 4 (Figure 1 and data not shown). According to the Kyte and Doolitle method (*36*), hydropathicity analysis of mouse NTPDase8 predicts two transmembrane domains in the polypeptide chain, one near the N terminus (amino acids 9−30) and one near the C terminus (amino acids 469−490; data not shown). Distance estimation of the amino acid sequences of various NTPDases and related proteins was performed with GeneBee (http://www.genebee.msu.su/). The phylogenetic tree obtained is shown in Figure 2. Murine NTPDase8 shares the highest homology with chicken ecto-ATPDase with 52.7% identity at the amino acid level (*38*, *39*).

RT-PCR analysis revealed that NTPDase8 mRNA is predominantly expressed in mouse liver. Lower levels of expression were detected in jejunum and kidney. A faint signal was also observed in lung, stomach, and testis (Figure 3). These results were confirmed by Northern blot analysis with total RNA, where a weak signal was obtained for liver and jejunum (data not shown).

Genomic Characterization of Entpd8. A homology search with the Mouse Sequence Data Base (www.ncbi.nih.gov/genome/seq/MmBlast.html) localized *Entpd8* to chromosome 2A3 (accession number NT_039205). Alignment of the full cDNA against the mouse genomic sequence reveals that mouse *Entpd8* covers approximately 5410 bp and is organized into 10 exons and 9 introns. All donor and acceptor splice sites conform to the GT/AG rule. Cloning of the genomic sequence of *Entpd8* from exon 2 to 10 confirmed the intron/exon junctions found in the above accession number (data not shown). The genomic structure of mouse *Entpd8* is summarized in Figure 4.

Biochemical Characterization of NTPDase8. The biochemical characteristics of this novel mammalian NTPDase were determined with crude cell lysates of COS-7 cells transiently transfected with an expression vector (pcDNA3.1/V5-His) containing the NTPDase8 cDNA. First, we determined the time course of nucleotide hydrolysis. The result in Figure 5A shows that the hydrolysis of ATP and ADP was linear from 5 to 30 min. All remaining assays were, therefore, carried out for 12−20 min. The effect of pH on ATPase and ADPase activity was then evaluated. Figure 5B shows that murine NTPDase8 was highly active between pH 4.0 and 8.0, with the optimal activity around pH 6.4 for ADPase activity. The enzyme showed a marked preference for Ca^{2+} over Mg^{2+} for the nucleotides tested (Figure 5C). In the presence of chelators of divalent cations, 1 mM EDTA and 1 mM EGTA, no activity could be detected with any of the substrates tested (data not shown). The substrate specificity of NTPDase8 in the presence of Ca^{2+} is shown in Figure 5D and Table 1. Although all triphospho- and diphosphonucleosides tested were hydrolyzed, NTPDase8 preferred triphosphonucleosides with a ratio on the order of ~2:1 (ATP/ADP = 1.6 ± 0.3 and UTP/UDP = 2.1 ± 0.3). Like other NTPDases, NTPDase8 does not hydrolyze AMP (Figure 5D, Table 1). As a control, the biochemical activity measured in untransfected COS-7 cell extracts was minimal,

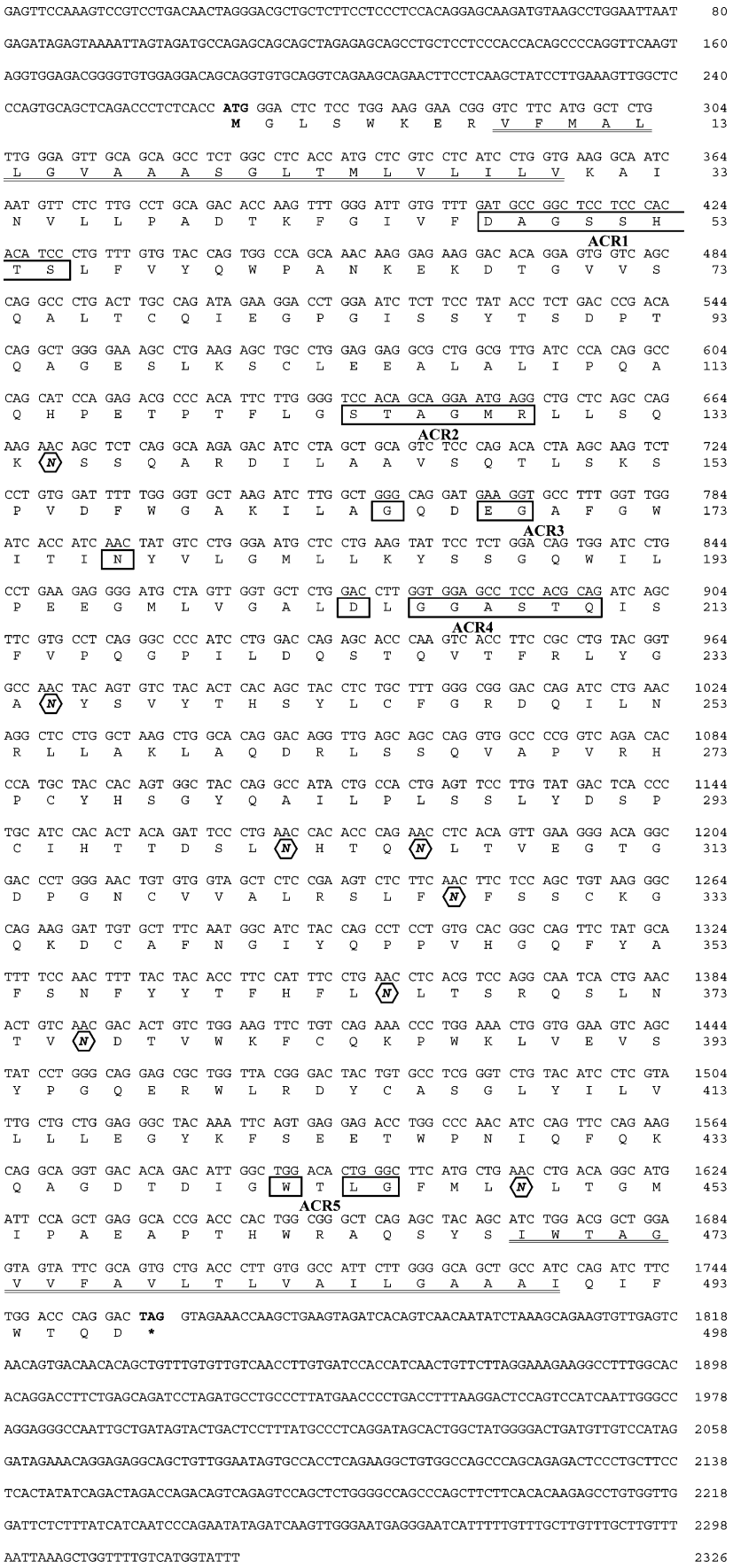

FIGURE 1: Nucleotide and predicted amino acid sequences of mouse NTPDase8 cDNA. The initiation codon and stop codon (indicated by an asterisk) are in bold face, and the potential N-glycosylation sites are presented by "*N*" surrounded by an hexagon. Two hydrophobic regions are double underlined, and the putative apyrase-conserved regions (ACR1−5) are boxed. Nucleotide sequences for both 5′ (1−178) and 3′ noncoding sections (1945−2326) were obtained from mouse ESTs (GenBank accession numbers BB610017 and AV026718, respectively).

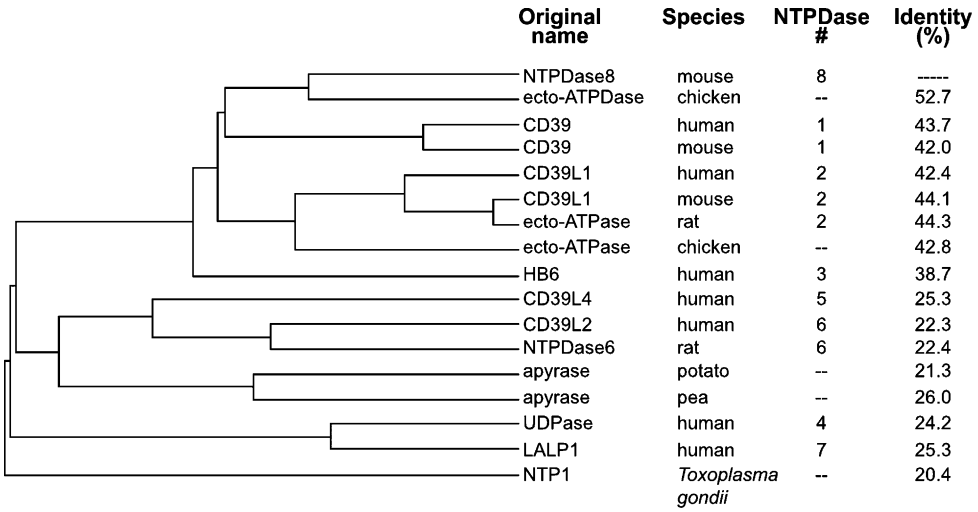

FIGURE 2: Phylogenetic analysis of amino acid sequences of selected NTPDases and related proteins. The percentage of amino acid identity of these proteins with mouse NTPDase8 was determined by pairwise alignment using ALIGN*p* (http://www.infobiogen.fr/services/analyseq/cgi-bin/alignp_in.pl). The GenBank accession numbers of the sequences are as follows: mouse NTPDase8, AY364442; chicken ecto-ATPDase, AF041355; human CD39L1, AF144748; mouse CD39L1, AF042811; rat ecto-ATPase, Y11835; chicken ecto-ATPase, U74467; human CD39, S73813; mouse CD39, AF037366; human HB6, AF034840; human CD39L4, AF039918; human CD39L2, AF039916; rat NTPDase6, AJ277748; potato apyrase, U58597; pea apyrase, Z32743; human UDPase, AF016032; human LALP1, AF269255; and *Toxoplasma gondii* apyrase, U96965.

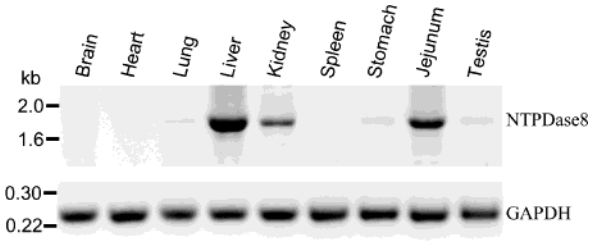

FIGURE 3: Tissue distribution of mouse NTPDase8 mRNA. RT-PCR was performed with total RNA from various mouse tissues. The PCR product of 1.78 kb, obtained with the 1st set of primers, was electrophoresed on a 1% agarose gel, stained with ethidium bromide, and photographed under UV. A GAPDH control giving a fragment of 240 bp is presented in the lower panel.

except at alkaline pHs. At pH 8.0, a maximum of 0.05 unit/mg of protein with ATP as a substrate was detected corresponding to less than 7% of the activity detected in transfected cells. Much lower contaminating activity was detected with the other substrates used.

All four nucleotides tested were hydrolyzed by NTPDase8 consistently with the Michaelis−Menten model of kinetics (Figure 6A for ATP; not shown for ADP, UTP, and UDP). The apparent K_m constants were calculated by plotting the data according to the Woolf−Augustinsson−Hofstee method (Figure 6A) and are summarized in Table 2. Triphosphonucleosides had lower apparent K_m values compared to their respective diphosphonucleoside by more than 3-fold, while the apparent V_{max} values were comparable in the four substrates tested. On the basis of these observations, it could be predicted that ATP and UTP hydrolysis by NTPDase8 would result in an accumulation of the corresponding diphosphoderivative. Because these intermediate products can also activate a subset of P2 receptors, we followed their accumulation by HPLC analysis over a time period of 2 h. Incubation of ATP or UTP with a crude cell lysate from NTPDase8 expressing COS-7 cells led to the formation of high levels of the corresponding diphosphonucleoside during the early phase of the reaction (parts B and C of Figure 6). In these experiments, ADP and UDP were further hydrolyzed to the corresponding monophosphonucleoside once the concentration of ATP and/or UTP had significantly decreased. After 120 min, ADP was completely hydrolyzed to AMP (Figure 6B), while UDP was still detectable at a concentration of 140 μM (Figure 6C). When both ATP and UTP were added together, adenine nucleotides were slightly preferentially hydrolyzed giving rise to an accumulation of

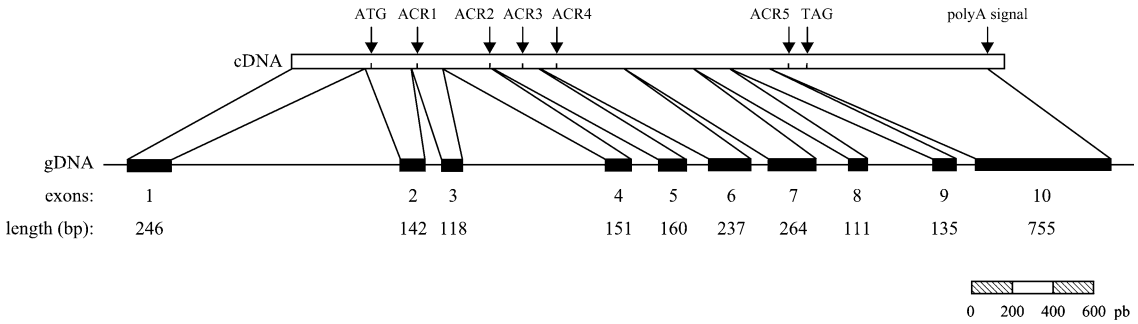

FIGURE 4: Schematic representation of the genomic organization of mouse *Entpd8*. The gene contains 10 exons that span a total of 5410 bp on mouse chromosome 2A3. The start and stop codons, the ACRs 1−5, as well as the polyA tail are indicated on the cDNA. Exons are presented by black boxes on the genomic DNA (gDNA), and their corresponding lengths are indicated.

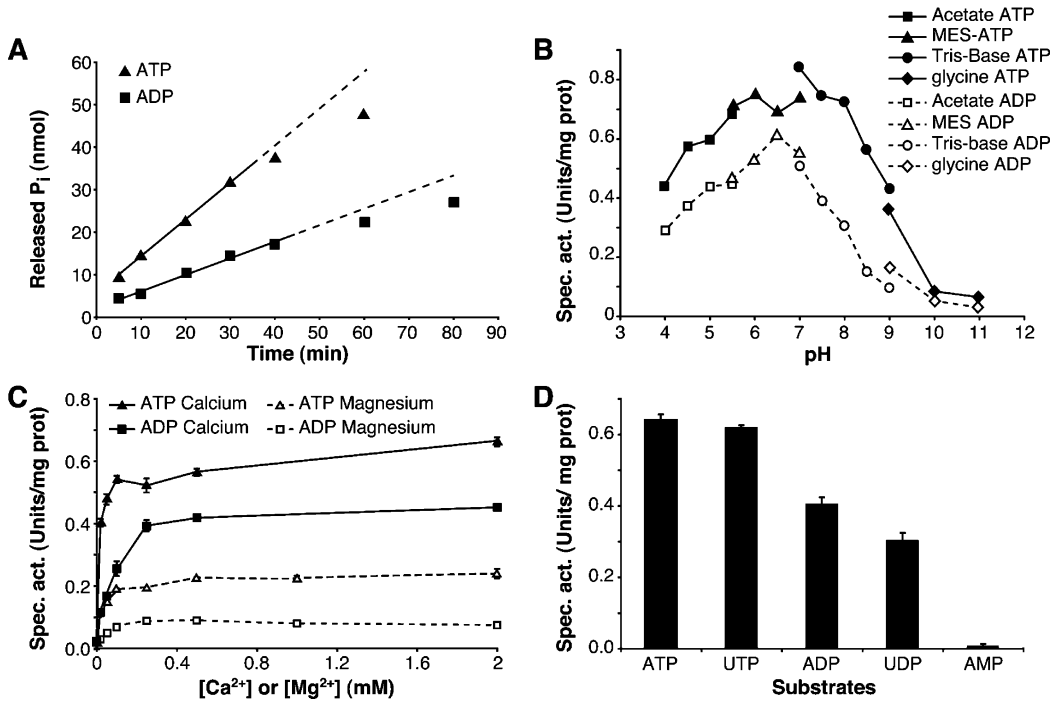

FIGURE 5: Biochemical characterization of mouse NTPDase8. Enzyme activity assays of crude cell lysates from NTPDase8 transfected COS-7 cells were carried out in 5 mM $CaCl_2$, 0.5 mM nucleotide (ATP, ADP, UTP, UDP, or AMP), and 100 mM Tris at pH 7.4 unless stated otherwise. In these experiments, less than 6% of the substrate was hydrolyzed. ATPase (▲) and ADPase (■) activities were assayed. For (A) and (B), a representative experiment of at least two independent experiments is shown. For (C) and (D), results are expressed as the mean ± standard deviation of the two independent experiments. Each individual experiment was performed 3 times. (A) Time course of nucleotide hydrolysis by NTPDase8. Reactions were linear from 5 to 30 min for both ATP and ADP as the substrates with an r^2 of more than 0.99. (B) Effect of pH. Four buffers [acetate, pH 4.0−5.5 (■, □); MES, pH 5.5−7.0 (▲, △); Tris, pH 7.0−9.0 (●, ○); and glycine, pH 9.0−11.0 (◆, ◇)] were used with ATP (solid symbols and solid lines) and ADP (open symbols and dotted lines) as the substrates. (C) Effect of Ca^{2+} and Mg^{2+} ions on the NTPDase activity. NTPDase8 was more active in the presence of Ca^{2+} (solid symbols and solid lines) than in the presence of Mg^{2+} (open symbols and dotted lines) with the ATPase (▲, △) activity being higher than the ADPase (■, □) activity for both cations. (D) Substrate specificity of NTPDase8.

Table 1: Substrate Specificity of Mouse NTPDase8 on Transiently Transfected Intact Cells[a]

	activity (nmol/min/well)	
substrate	COS-7 cells	293T cells
ATP	3.77 ± 0.14	3.55 ± 0.15
ADP	1.06 ± 0.07	1.54 ± 0.23
UTP	2.17 ± 0.08	2.34 ± 0.31
UDP	0.48 ± 0.04	0.72 ± 0.04
AMP	ND	ND

[a] The appearance of enzymatic activity at the surface of intact COS-7 and 293T cells transfected with an expression vector containing mouse NTPDase8 was measured in 24-well plates in the presence of 5 mM $CaCl_2$, 145 mM NaCl, 0.5 mM nucleotide, and 100 mM Tris at pH 7.4. The activity obtained with the control cells was subtracted from the one obtained with NTPDase8 transfected cells. Each individual experiment was performed 3 times. A representative experiment of three to six independent experiments is shown. Results are expressed as the mean ± standard deviation. No activity could be detected with AMP (ND = not detected). Statistical analysis confirmed that the activity of intact transfected cells was significantly higher than the activity of untransfected control cells for all four substrates ($P < 0.005$).

UDP for an important period of time (Figure 6D). These data are in agreement with the lower K_m values for adenine nucleotides compared to those for uracil nucleotides. Similar patterns of hydrolysis were observed with confluent intact COS-7 cells transiently transfected with NTPDase8 (data not shown).

In addition, the tight association of NTPDase8 with the membrane fraction was confirmed by an ultracentrifugation of the crude cell lysate at 100000*g* for 1 h. Indeed, more than 90% of the total ATPase and ADPase activities were found in the pellet fraction (data not shown). Altogether, these experiments demonstrate that mouse NTPDase8 is an ectoenzyme tightly bound to the plasma membrane.

DISCUSSION

This paper reports the identification of a novel member of the mammalian E-NTPDase family. Genomic analysis using the mouse NTPDase8 cDNA sequence showed that *Entpd8* is localized on chromosome 2A3 and is comprised of 10 exons. Hence, it is distinct from genes encoding other murine NTPDases located on chromosome 19C3, 2A3, 9F4, 14D1, 12D1, 2G3, and 19C3 for *Entpd1*−*7*, respectively (data not shown); *Entpd8* maps 306 kb upstream of *Entpd2* on the same chromosome. A search of the NCBI database reveals the presence of a human gene on chromosome 9 that is homologous to mouse *Entpd8*. ESTs from the pancreas and stomach (e.g., GenBank accession number BI793151) confirm that the human gene is functional.

Among mammalian NTPDases, NTPDase8 shares the highest homology with NTPDase1−3 with a predicted amino acid identity ranging from 38% to 48% (Figure 2 and data not shown). NTPDase8 had lower homology with intracellular NTPDases (members 4−7) with about 22−25% identity. A 53% amino acid identity was found with the nonmammalian chicken ecto-ATPDase (*38*, *39*). NTPDase8 shares other important characteristics with NTPDase1−3, including two transmembrane domains with short intracytoplasmic sequences at both ends (N and C termini), a

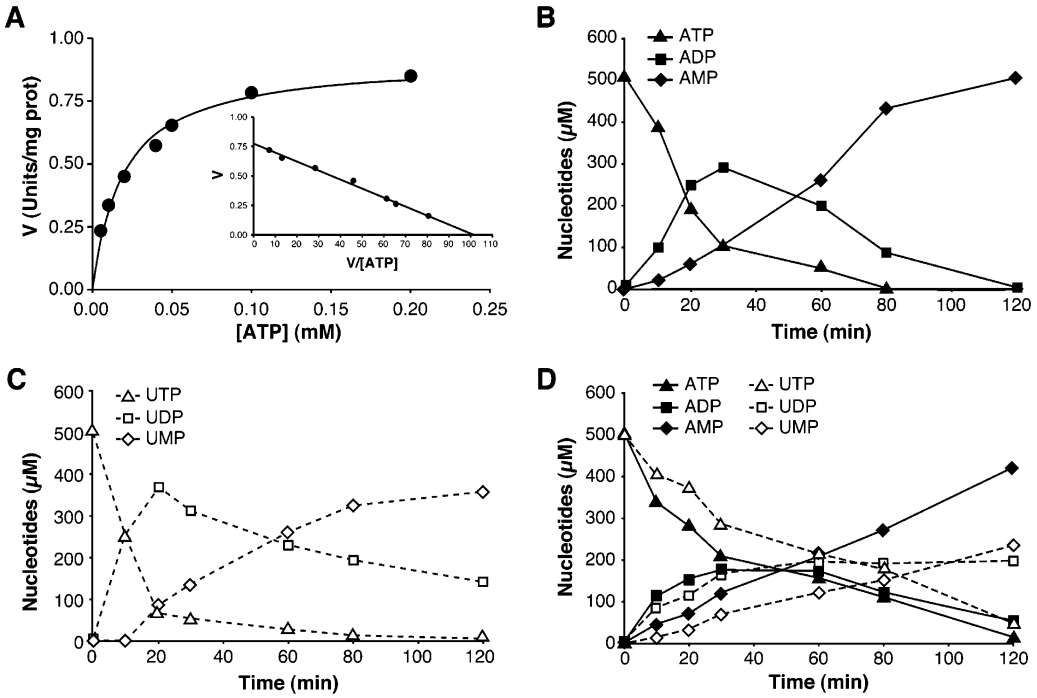

FIGURE 6: Kinetics and profiles of nucleotide hydrolysis of mouse NTPDase8. For (A), reactions were carried out for 12 min in the presence of 5 mM $CaCl_2$ and 100 mM MES at pH 6.4. The average of three separate experiments each performed 3 times is presented. Graphs were produced using GraphPad Prism (GraphPad Software Inc., San Diego, CA). For the analysis of ATP and UTP hydrolysis products (B−D), the reaction was started by the addition of 5 μL of NTPDase8 crude cell lysate (~6 μg) to the reaction mixture containing 0.5 mM ATP and/or UTP. Aliquots were taken at different time points, and the reaction was stopped immediately by the addition of an equal volume of ice-cold 1 M perchloric acid. These samples were deproteinated, lipids were removed, and the nucleotide content was analyzed by HPLC as described in the Experimental Procedures. (A) Michaelis−Menten data representation of ATP concentration ranging from 5 to 200 μM. Inset, Woolf−Augustinsson−Hofstee plot was used to evaluate the apparent K_m and V_{max}. Kinetic parameters are summarized in Table 2. (B) Time course of ATP hydrolysis by a murine NTPDase8 crude cell lysate: ATP (▲), ADP (■), and AMP (◆). (C) UTP hydrolysis by a NTPDase8 crude cell lysate: UTP (△), UDP (□), and UMP (◇). (D) Simultaneous hydrolysis of ATP and UTP by NTPDase8: ATP (▲), ADP (■), AMP (◆), UTP (△), UDP (□), and UMP (◇).

Table 2: Kinetic Constants of NTPDase8[a]

substrate	$K_{m,app}$ (μM)	$V_{max,app}$ (unit/mg of protein)
ATP	13 ± 6	0.82 ± 0.02
ADP	41 ± 6	0.95 ± 0.08
UTP	47 ± 1	1.13 ± 0.02
UDP	171 ± 15	1.08 ± 0.06

[a] Apparent K_m and V_{max} values ($K_{m,app}$, $V_{max,app}$) were estimated by regression analysis of Woolf−Augustinsson−Hofstee plots. Results obtained with COS-7 crude cell lysates are expressed as the mean ± standard error of the mean of three independent experiments, each performed 3 times. The curves drawn from these data gave an r^2 of 0.99, 0.98, 0.99, and 0.96 for ATP, ADP, UTP, and UDP, respectively.

tight association with the plasma membrane, a high level of glycosylation (>6 potential N-glycosylation sites), and an active site facing the extracellular milieu (Figure 1). The latter was confirmed by the appearance of nucleotidase activity on transiently transfected intact COS-7 and 293T cells (Table 1).

Because of their membrane topology, NTPDase1−3, and -8 are ectoenzymes that dephosphorylate nucleotides in the extracellular compartment. There are some similarities between the biochemical properties of these enzymes, as well as important differences. While NTPDase2 prefers triphospho- over diphosphonucleoside by about 30-fold (*7*, *26*), NTPDase1, -3, and -8 catalyze the hydrolysis of triphospho- and diphosphonucleosides efficiently with ATP:ADP rates of hydrolysis of ~1:1 (*40*), ~3:1 (*11*, *41*, *42*), and ~2:1, respectively. The intermediate products generated by plasma membrane bound NTPDases accumulate in a different manner. NTPDase1 hydrolyzes ATP sequentially, leading to the formation of AMP with the liberation of two molecules of inorganic phosphate; ADP is released from the catalytic site in minute amounts (*7*, *43*). In contrast, NTPDase2 accumulates ADP in the reaction medium (*7*, *26*). Interestingly, in the presence of ATP, NTPDase8 leads to the transient accumulation of ADP (Figure 6B). ADP levels are reduced only when the ATP concentration had significantly decreased. Similar data were obtained with UTP as the substrate (parts C and D of Figure 6). Consistent with these observations, NTPDase8 has apparent K_m values in the low micromolar range with a preference for triphosphonucleosides compared to diphosphonucleosides, as well as for adenine nucleotides over uracil nucleotides. In comparison, ATP and ADP have similar affinity toward NTPDase1 with apparent K_m values on the order of 10 μM (*43*, *44*). Human NTPDase2 from NIH-3T3 stably transfected cells was reported to have apparent K_m values around 400 μM for ATP and 100 μM for ADP with apparent V_{max} values of 107 nmol of P_i min^{-1} $(10^6$ cells$)^{-1}$ for ATP and 4 nmol of P_i min^{-1} $(10^6$ cells$)^{-1}$ for ADP (*8*). The apparent K_m values of human NTPDase3, evaluated from crude cell lysates of transfected COS-1 cells, were 128 and 96 μM and apparent V_{max} values of 2.0 units/mg of protein and 0.5 unit/mg of protein for ATP and ADP, respectively (*41*). Another interesting particularity of NTPDase8 is its relatively high activity between pH 4.0 and 8.0, with an optimal activity between pH 5.5 and 8.0.

The biochemical and kinetic information presented in this paper suggest that NTPDase8 would modulate the concentration of nucleotides/nucleosides in a different manner than other plasma membrane bound NTPDases and would therefore affect P2-receptor signaling distinctly. For example, the relatively high accumulation of ADP and UDP observed in parts B−D of Figure 6, in agreement with the apparent K_m values, suggests that NTPDase8 would not only limit the activation of receptors preferentially activated by ATP and/or UTP such as $P2X_{1-7}$ and $P2Y_{2,4,11}$ (*29*, *31*, *45*) but also favor the transient activation of ADP- and UDP-specific receptors such as $P2Y_{1,6,12,13}$ (*29*, *30*). The latter property is expected to be partly shared by NTPDase2 (*26*). However, in contrast to NTPDase2, NTPDase8 facilitates the late appearance of adenosine, generated by the hydrolysis of AMP by ecto-5′-nucleotidase (*46*). Because the latter enzyme is inhibited by ATP and ADP, the formation of adenosine would then be expected to be further delayed in the presence of NTPDase8, generating a gap between the activation of P2 receptors and the subsequent activation of adenosine receptors. These steps reflect the fact that ATP is the major nucleotide secreted by cells (*47*). In similar circumstances, NTPDase1 would be expected to promote a faster generation of adenosine because it favors the rapid formation of AMP. Together, the above observations suggest that NTPDases tightly regulate nucleotide levels, thereby controlling P2-receptor activation. In concert with the ecto-5′-nucleotidase, NTPDases contribute to the formation of adenosine, a biologically active molecule that acts via its own specific receptors (*27*, *32*).

In summary, a novel mammalian plasma membrane bound NTPDase has been identified, and its kinetic properties have been described. This enzyme is expected to regulate extracellular nucleotide levels in a manner distinct from that of other ectonucleotidases hitherto described, providing an alternative avenue of regulating cell functions meditated by nucleotides and nucleosides.

ACKNOWLEDGMENT

We are grateful to Mrs. Julie Pelletier for her technical assistance and to Dr. Guy Poirier from the research unit “Santé et environnement” of the CHUL research center for providing the COS-7 cell line.

REFERENCES

1. Zimmermann, H. (2001) Ectonucleotidases: Some recent developments and note on nomenclature, *Drug Dev. Res. 52*, 44−56.
2. Mulero, J. J., Yeung, G., Nelken, S. T., and Ford, J. E. (1999) CD39-L4 is a secreted human apyrase, specific for the hydrolysis of nucleoside diphosphatases, *J. Biol. Chem. 274*, 20064−20067.
3. Wang, T.-F., and Guidotti, G. (1996) CD39 is an ecto-(Ca^{2+}, Mg^{2+})-apyrase, *J. Biol. Chem. 271*, 9898−9901.
4. Kaczmarek, E., Koziak, K., Sévigny, J., Siegel, J. B., Anrather, J., Beaudoin, A. R., Bach, F. H., and Robson, S. C. (1996) Identification and characterization of CD39 vascular ATP diphosphohydrolase, *J. Biol. Chem. 271*, 33116−33122.
5. Sévigny, J., Lévesque, F. P., Grondin, G., and Beaudoin, A. R. (1997) Purification of the blood vessel ATP diphosphohydrolase, identification and localization by immunological techniques, *Biochim. Biophys. Acta 1334*, 73−88.
6. Chadwick, B. P., and Frischauf, A. M. (1997) Cloning and mapping of a human and mouse gene with homology to ecto-ATPase genes, *Mamm. Genome 8*, 668−672.
7. Heine, P., Braun, N., Heilbronn, A., and Zimmermann, H. (1999) Functional characterization of rat ecto-ATPase and ecto-ATP diphosphohydrolase after heterologous expression in CHO cells, *Eur. J. Biochem. 262*, 102−107.
8. Mateo, J., Harden, T. K., and Boyer, J. L. (1999) Functional expression of a cDNA encoding a human ecto-ATPase, *Br. J. Pharmacol. 128*, 396−402.
9. Vlajkovic, S. M., Housley, G. D., Greenwood, D., and Thorne, P. R. (1999) Evidence for alternative splicing of ecto-ATPase associated with termination of purinergic transmission, *Mol. Brain Res. 73*, 85−92.
10. Chadwick, B. P., and Frischauf, A. M. (1998) The CD39-like gene family−Identification of three new human members (CD39L2, CD39L3, and CD39L4), their murine homologues, and a member of the gene family from *Drosophila melanogaster*, *Genomics 50*, 357−367.
11. Smith, T. M., and Kirley, T. L. (1998) Cloning, sequencing, and expression of a human brain ecto-apyrase related to both the ecto-ATPases and CD39 ecto-apyrases, *Biochim. Biophys. Acta 386*, 65−78.
12. Wang, T. F., and Guidotti, G. (1998) Golgi localization and functional expression of human uridine diphosphatase, *J. Biol. Chem. 273*, 11392−11399.
13. Biederbick, A., Kosan, C., Kunz, J., and Elsasser, H. P. (2000) First apyrase splice variants have different enzymatic properties, *J. Biol. Chem. 275*, 19018−19024.
14. Trombetta, E. S., and Helenius, A. (1999) Glycoprotein reglucosylation and nucleotide sugar utilization in the secretory pathway: identification of a nucleoside diphosphatase in the endoplasmic reticulum, *EMBO J. 18*, 3282−3292.
15. Paez, J. G., Recio, J. A., Rouzaut, A., and Notario, V. (2001) Identity between the PCPH proto-oncogene and the CD39L4 (ENTPD5) ectonucleoside triphosphate diphosphohydrolase gene, *Int. J. Oncol. 19*, 1249−1254.
16. Yeung, G., Mulero, J. J., McGowan, D. W., Bajwa, S. S., and Ford, J. E. (2000) CD39L2, a gene encoding a human nucleoside diphosphatase, predominantly expressed in the heart, *Biochemistry 39*, 12916−12923.
17. Hicks-Berger, C. A., Chadwick, B. P., Frischauf, A. M., and Kirley, T. L. (2000) Expression and characterization of soluble and membrane-bound human nucleoside triphosphate diphosphohydrolase 6 (CD39L2), *J. Biol. Chem. 275*, 34041−34045.
18. Braun, N., Fengler, S., Ebeling, C., Servos, J., and Zimmermann, H. (2000) Sequencing, functional expression and characterization of rat NTPDase6, a nucleoside diphosphatase and novel member of the ecto-nucleoside triphosphate diphosphohydrolase family, *Biochem. J. 351*, 639−647.
19. Shi, J. D., Kukar, T., Wang, C. Y., Li, Q. Z., Cruz, P. E., Davoodi-Semiromi, A., Yang, P., Gu, Y., Lian, W., Wu, D. H., and She, J. X. (2001) Molecular cloning and characterization of a novel mammalian endo-apyrase (LALP1), *J. Biol. Chem. 276*, 17474−17478.
20. Miura, Y., Hirota, K., Arai, Y., and Yagi, K. (1987) Purification and partial characterization of adenosine diphosphatase activity in bovine aorta microsomes, *Thromb. Res. 46*, 685−695.
21. Côté, Y. P., Filep, J. G., Battistini, B., Gauvreau, J., Sirois, P., and Beaudoin, A. R. (1992) Characterization of ATP-diphosphohydrolase activities in the intima and media of the bovine aorta: evidence for a regulatory role in platelet activation in vitro, *Biochim. Biophys. Acta 1139*, 133−142.
22. Marcus, A. J., Broekman, M. J., Drosopoulos, J. H. F., Islam, N., Alyonycheva, T. N., Safier, L. B., Hajjar, K. A., Posnett, D. N., Schoenborn, M. A., Schooley, K. A., Gayle, R. B., and Maliszewski, C. R. (1997) The endothelial cell ecto-ADPase responsible for inhibition of platelet function is CD39, *J. Clin. Invest. 99*, 1351−1360.
23. Enjyoji, K., Sévigny, J., Lin, Y., Frenette, P. S., Christie, P. D., Schulte Am Esch, J., II, Imai, M., Edelberg, J. M., Rayburn, H., Lech, M., Beeler, D. L., Csizmadia, E., Wagner, D. D., Robson, S. C., and Rosenberg, R. D. (1999) Targeted disruption of CD39/ATP diphosphohydrolase results in disordered hemostasis and thromboregulation, *Nat. Med. 5*, 1010−1017.
24. Pinsky, D. J., Broekman, M. J., Peschon, J. J., Stocking, K. L., Fujita, T., Ramasamy, R., Connolly, E. S., Jr., Huang, J., Kiss, S., Zhang, Y., Choudhri, T. F., McTaggart, R. A., Liao, H., Drosopoulos, J. H., Price, V. L., Marcus, A. J., and Maliszewski, C. R. (2002) Elucidation of the thromboregulatory role of CD39/ectoapyrase in the ischemic brain, *J. Clin. Invest. 109*, 1031−1040.
25. Mizumoto, N., Kumamoto, T., Robson, S. C., Sévigny, J., Matsue, H., Enjyoji, K., and Takashima, A. (2002) CD39 is the dominant

Langerhans cell-associated ecto-NTPDase: Modulatory roles in inflammation and immune responsiveness, *Nat. Med. 8*, 358−365.
26. Sévigny, J., Sundberg, C., Braun, N., Guckelberger, O., Csizmadia, E., Qawi, I., Imai, M., Zimmermann, H., and Robson, S. C. (2002) Differential catalytic properties and vascular topography of murine nucleoside triphosphate diphosphohydrolase 1 (NTPDase1) and NTPDase2 have implications for thromboregulation, *Blood 99*, 2801−2809.
27. Klinger, M., Freissmuth, M., and Nanoff, C. (2002) Adenosine receptors: G protein-mediated signaling and the role of accessory proteins, *Cell. Signalling 14*, 99−108.
28. Dubyak, G. R., and Elmoatassim, C. (1993) Signal transduction via P2-purinergic receptors for extracellular ATP and other nucleotides, *Am. J. Physiol. 265*, C577−C606.
29. Muller, C. E. (2002) P2-pyrimidinergic receptors and their ligands, *Curr. Pharm. Des. 8*, 2353−2369.
30. Abbracchio, M. P., Boeynaems, J. M., Barnard, E. A., Boyer, J. L., Kennedy, C., Miras-Portugal, M. T., King, B. F., Gachet, C., Jacobson, K. A., Weisman, G. A., and Burnstock, G. (2003) Characterization of the UDP-glucose receptor (renamed here the P2Y14 receptor) adds diversity to the P2Y receptor family, *Trends Pharmacol. Sci. 24*, 52−55.
31. North, R. A. (2002) Molecular physiology of P2X receptors, *Physiol. Rev. 82*, 1013−1067.
32. Fredholm, B. B., AP, I. J., Jacobson, K. A., Klotz, K. N., and Linden, J. (2001) International Union of Pharmacology. XXV. Nomenclature and classification of adenosine receptors, *Pharmacol. Rev. 53*, 527−552.
33. Heyer, B. S., MacAuley, A., Behrendtsen, O., and Werb, Z. (2000) Hypersensitivity to DNA damage leads to increased apoptosis during early mouse development, *Genes Dev. 14*, 2072−2084.
34. Chapdelaine, P., Delahaye, S., Gauthier, E., Tremblay, R. R., and Dube, J. Y. (1993) A one-hour procedure for the preparation of genomic DNA from frozen tissues, *BioTechniques 14*, 163−164.
35. Bradford, M. M. (1976) A rapid and sensitive method for quantification of microgram quantities of protein utilizing the principle of protein-dye binding, *Anal. Biochem. 72*, 248−254.
36. Baykov, A. A., Evtushenko, O. A., and Avaeva, S. M. (1988) A malachite green procedure for orthophosphate determination and its use in alkaline phosphatase-based enzyme immunoassay, *Anal. Biochem. 171*, 266−270.
37. LeBel, D., Poirier, G. G., Phaneuf, S., St, J. P., Laliberté, J. F., and Beaudoin, A. R. (1980) Characterization and purification of a calcium-sensitive ATP diphosphohydrolase from pig pancreas, *J. Biol. Chem. 255*, 1227−1233.
38. Nagy, A. K., Knowles, A. F., and Nagami, G. T. (1998) Molecular cloning of the chicken oviduct ecto-ATP-diphosphohydrolase, *J. Biol. Chem. 273*, 16043−16049.
39. Knowles, A. F., Nagy, A. K., Strobel, R. S., and Wu-Weis, M. (2002) Purification, characterization, cloning, and expression of the chicken liver ecto-ATP-diphosphohydrolase, *Eur. J. Biochem. 269*, 2373−2382.
40. Beaudoin, A. R., Sévigny, J., and Picher, M. (1996) in *ATPases* (Lee, A. G., Ed.) pp 369−401, JAI Press Inc., Greenwich, CT.
41. Smith, T. M., and Kirley, T. L. (1999) Site-directed mutagenesis of a human brain ecto-apyrase: Evidence that the E-type ATPases are related to the actin/heat shock 70/sugar kinase superfamily, *Biochemistry 38*, 321−328.
42. Lavoie, É. G., Kukulski, F., Lévesque, S. A., Lecka, J., and Sévigny, J. (2004) Cloning and characterization of mouse nucleoside triphosphate diphosphohydrolase-3, *Biochem. Pharmacol.* in press.
43. Laliberté, J. F., and Beaudoin, A. R. (1983) Sequential hydrolysis of the γ- and β-phosphate groups of ATP by the ATP diphosphohydrolase from pig pancreas, *Biochim. Biophys. Acta 742*, 9−15.
44. Picher, M., Sévigny, J., D'Orleans-Juste, P., and Beaudoin, A. R. (1996) Hydrolysis of P2-purinoceptor agonists by a purified ectonucleotidase from the bovine aorta, the ATP-diphosphohydrolase, *Biochem. Pharmacol. 51*, 1453−1460.
45. White, P. J., Webb, T. E., and Boarder, M. R. (2003) Characterization of a Ca^{2+} response to both UTP and ATP at human P2Y11 receptors: evidence for agonist-specific signaling, *Mol. Pharmacol. 63*, 1356−1363.
46. Zimmermann, H. (1992) 5′-nucleotidase: molecular structure and functional aspects, *Biochem. J. 285*, 345−365.
47. Bodin, P., and Burnstock, G. (2001) Purinergic signalling: ATP release, *Neurochem. Res. 26*, 959−969.

BI0362222